Post-15th century European glass beads in southern Africa: Composition and classification using pXRF and Raman spectroscopy

Farahnaz Koleini [a,*], Philippe Colomban [b], Innocent Pikirayi [a]

[a] Department of Anthropology and Archaeology, Faculty of Humanities, University of Pretoria, Pretoria, Gauteng, South Africa

[b] Sorbonne Université, CNRS, MONARIS UMR8233, 4 Place Jussieu, 75005 Paris, France

* Corresponding author. E-mail address: farakoleini@gmail.com (F. Koleini).

Highlights

- We classified European glass beads traded to southern Africa since the 16th c.
- The glass beads were analysed by using Raman micro-spectroscopy and pXRF.
- Six different groups were recorded.
- Six sub-groups were recorded.
- The composition of glass and pigments suggested the dates and provenances of them.

Abstract

A hundred and twenty-seven glass beads found at the archaeological sites in southern Africa were analysed using pXRF and Raman spectroscopy. The beads are identified as European productions on the basis of their composition and morphology. Six identified glass groups are soda-based plant ash (61%), potash-rich wood ash (14%), synthetic soda (8%), mixed alkali (4%), lead-soda (22%) and natron (4%). Except for soda-based plant ashes and natron (outliers), all the groups date back to the 19th century. Calcium antimonate ($Ca_2Sb_2O_7$) detected in most of the soda-based plant ash glasses (87%) indicated that some of the beads had been imported from Europe since the 17th century.

Keywords

Trade glass beads; Provenance; Europe; Pigments; southern Africa

1. Introduction: An historical perspective

Glass beads have been produced and traded to southern Africa for use as everyday items of adornment, ceremonial costumes or objects of barter since the 7th century. The preservation of glass beads is good and large hoards have been found in archaeological sites. Till now, 7 series of bead with different compositions are detected among traded beads to southern Africa before the 18th century (Wood, 2011, Wood et al., 2012). These beads are mainly monochrome and all, except Mapungubwe and Zimbabwe series which their origin is not clear yet, imported from Asia. A summary of these bead series are presented in Table S1. However, European producers have copied the shapes and colours of the ancient beads, highly prized by the African communities, which makes their identification difficult using morphological criteria (Koleini et al., 2019a, Wood, 2008).

The history of glass making in the Mediterranean region shows that the mineral flux (natron) was in use from the Roman times until about the 10th century CE (Freestone et al., 2000, Gratuze, 2013). Natron was completely replaced with Levantine ash in Venice during the 14th century (Shortland et al., 2006). Indeed, Levantine ash was produced by burring of *Salsola soda* plant species and was being used in Venice and Italy (Tuscan, Savona) in the production of glass from the 10th century onwards (Cagno et al., 2010, Cagno et al., 2012, De Raedt et al., 2001). Later on, in the 17th century, Levantine ash was gradually replaced by other West Mediterranean coastal ashes because it was no longer exported to Europe from the Levant (Verità and Zecchin, 2009). Barilla ash was produced by burning coastal plants (*Salsola kali*) growing in various places in the West Mediterranean (Cagno et al., 2010). Barilla, along with Levantine ash, was employed in glass production from the 13th century until the 17th century (Cagno et al., 2012, Verità and Zecchin, 2009) (see summary in Table S2). Barilla ash can be differentiated from Levantine ash by its higher K_2O content (>5 wt%) than Levantine ash (<4 wt%) (Cagno et al., 2012, Tite et al., 2006).

From the 16th century onwards, very close glass compositions to Venetian productions, known as *Façon-de-Venise* were produced in other parts of Europe with the movement of Italian glassmakers (De Raedt et al., 2002). After the late 17th century, pure potassium ash glass found in Central Europe and lead-based glass in Britain, started to be produced (Coutinho, 2016). Pure potassium-lime silica glass was also being produced by mixing purified wood ash with other very pure raw minerals (Kunicki-Goldfinger et al., 2005). Finally, in the 19th century, plant ash was replaced by synthetic soda and potash in Central Europe (Dungworth, 2011).

The first European glass beads were brought to southern Africa by Portuguese traders in the 15th century CE (Koleini et al., 2019a, Koleini et al., 2019b). Wood (2011) mentioned that these beads were rejected by native Africans due to their unfamiliar appearance when compared to the beads (Asian beads) used by their ancestors. This has led the traders to continue bringing South and South-East Asian beads to southern Africa instead. These glass beads are known as Khami Indo Pacific series and were imported from the 15th to the 17th centuries (Koleini et al., 2019a, Koleini et al., 2019b). However, beads assigned to European origins are generally found alongside with Khami bead series at the very top layers of archaeological sites (Koleini et al., 2017). These European beads were presumably imported via Dutch and British trading posts to southern African inland after the 17th century while some pre-European beads found with the European ones could be heirlooms.

Some annular and hexagonal as well as opaque white European beads can easily be discriminated by visual examination from the pre-European series found in southern Africa sites. However, some of the monochrome drawn beads look very similar in morphology to the former Asian series (Koleini et al., 2016a). Accordingly, it is possible that some beads such as the simple brownish-red and black ones, were imported earlier from Europe and distributed along with the beads of the Khami series in southern Africa. These beads might be differentiated on the basis of their composition, pigments and opacifiers.

Morphology, composition and pigments can be used as criteria for dating European glass beads (Koleini et al., 2019a). For the preservation of these artefacts, non-invasive analysis is needed. In the present paper, the composition of European glass beads (Fig. 1) found at

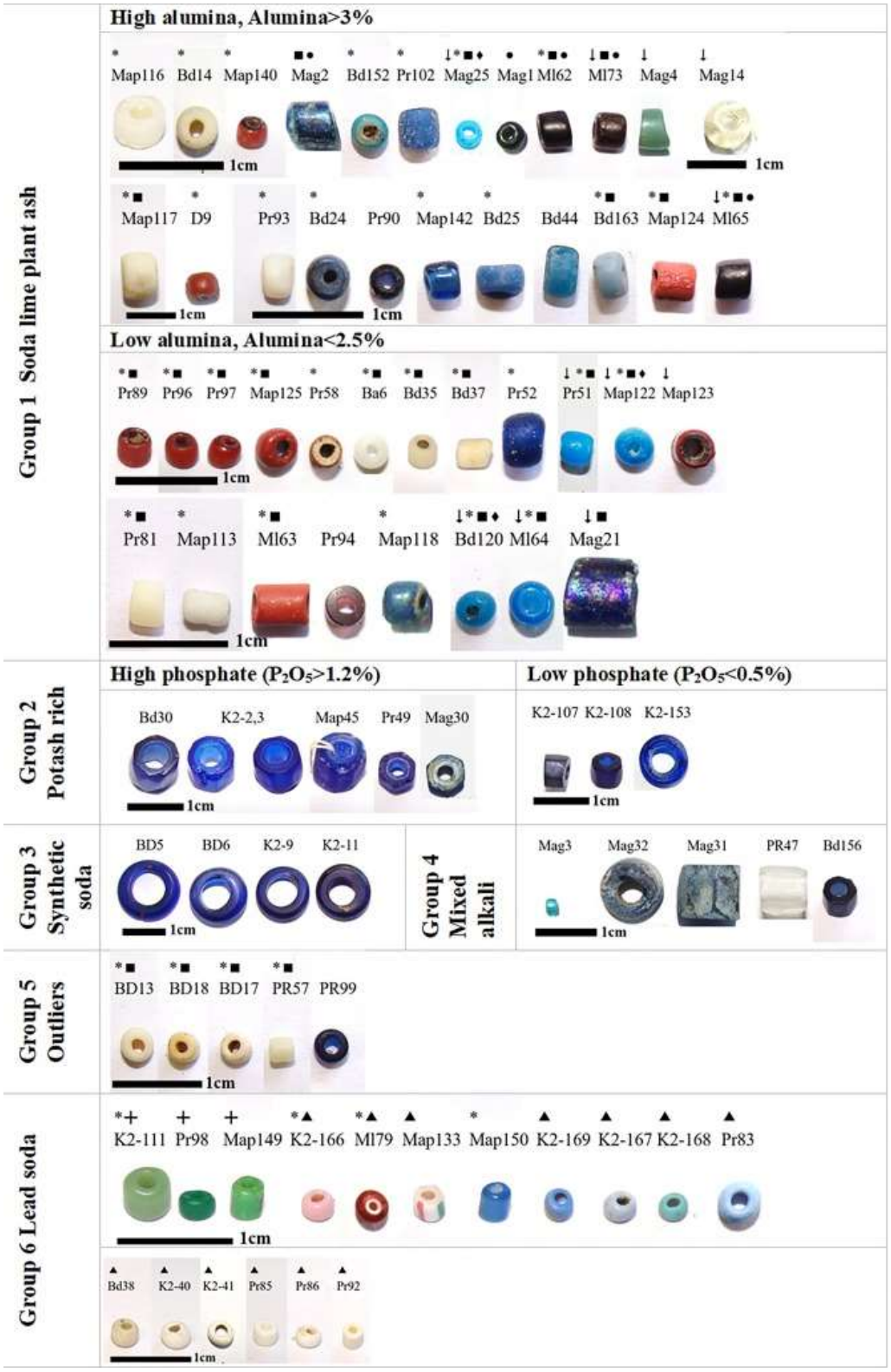

Fig. 1. Representative analysed beads classified in 6 different compositional groups. ↓ = Low lime (pure ash), *=Calcium antimoniate ($Ca_2Sb_2O_7$), ■=Lead < 13%, ●=Manganese, ▲=Arsenate, +=Pb-Sn-Sb triple oxides, ♦=Lazurite.

Mapungubwe, Bambandyanalo, Parma and Maryland farms in northern South Africa were examined using portable XRF (pXRF). The results are compared with the similar European beads which were found at Magoro Hill in South Africa, Danamombe and Baranda in Zimbabwe (Koleini et al., 2016a, Koleini et al., 2017, Koleini et al., 2019b) (Figure S1). Then, the results were associated with the recorded Raman data of beads available in the studies of Tournié et al., 2012, Koleini et al., 2016a which included the samples from K2, Mapungubwe and Magoro Hill sites. Portable XRF is widely used for material characterization in different domains, namely geology, environment, pollution, agriculture and specifically cultural heritage due to its non-destructive character (Rostron and Ramsey, 2017, Peinado et al., 2010, Craig et al., 2007, Zhao and Li, 2017). Mobile Raman micro-spectroscopy is also a non-destructive technique which can be used as complementarily with pXRF for the classification of glass beads at archaeological sites (Simsek et al. 2015). Finally, the beads were classified and dated by considering the glass production sequence in Europe.

We present here a systematic classification of the European beads traded to southern Africa on the basis of morphology and composition. These items were hardly discussed thoroughly by previous researchers who mainly focused on the pre-colonial period. With the identification of the composition of beads, the earlier Asian monochrome drawn beads can be separated from European replicas. Furthermore, it would be a starting point for collecting information on extent and distribution model of different exotic beads in southern Africa after the arrival of the Europeans.

2. Materials and methods

2.1. Samples and archaeological context

127 European glass beads lounged at University of Pretoria Museum and coming from southern Africa archaeological sites (Fig. 1) were classified according to morphology (Table S3) and material composition (Table 1 and S2). 105 of these beads were excavated at Parma (Pr), Maryland (Ml), Mapungubwe (Map), Bambandyanlo (Bd) and K2 sites in the Limpopo valley, South Africa (Figure S1). Thirty-five beads from Mapungubwe and Bambandyanalo were previously examined by Raman spectroscopy (Prinsloo et al., 2011, Tournié et al., 2012). The already published XRF and Raman results of European beads from Magoro Hill (Mag) (13 beads) in South Africa, Baranda (Ba) (1 bead) and Danamombe (D) (8 beads) in Zimbabwe (Koleini et al., 2016a, Koleini et al., 2017, Koleini et al., 2019b] were also evaluated for comparative purposes. The samples are labelled with the acronym of the site followed by XRF test number of the beads as reported in Fig. 1.

Bambandyanalo and the adjacent test excavation location (K2) (10th-11th century), Mapungubwe (13th century), Parma and Maryland sites (dates not well established) are located along the middle Limpopo River and close to the current borders of Zimbabwe, Botswana and South Africa. All the sites were homesteads of Iron-Age farmers during the early second millennium AD. In the case of Bambandyanalo and Mapungubwe, there is no further evidence of large occupancy of the sites following their abandonment after the 11th and the 13th century respectively (Huffman, 2000). Therefore, European beads found at these two sites probably belong to later human activity which continued up to the mid-19th century (Prinsloo et al., 2011). Ceramics and glass finds from the preliminary excavation in Parma shows that the occupation started with the Bambandyanalo phase and continued with a later one with an interval between two phases (Fouché, 1937). Three packets of glass beads are

attributed to Parma in the University of Pretoria Museum. The information on the packets refers to three locations as Parma midden, Parma X1 and Parma. Fouché (1937) reported that Maryland was occupied for a short period and consisted of a shallow deposit. Beads were collected from two locations, close to the stone wall and a cattle pen next to the main site. The occupation date of the site is not clear.

2.2. Analytical methods

X-ray fluorescence spectroscopy was performed by using a handheld Niton Thermo Scientific XL3t GOLDD. The amounts of 36 elements with atomic numbers higher than sodium were measured by using the fundamental parameters as employed in Mining Cu/Zn modes. The details of the instrument and the analysis procedure were reported previously (Koleini et al., 2016b). The elements measured by XRF were converted into oxide forms and then normalized to 100%. Due to the limitation in the measuring of low Z-elements using the pXRF instrument, standard glass samples B, C and D from Corning Museum of Glass were used as reference to obtain (semi-) quantitative data. Each reference was analysed three times and the normalisation factor was calculated by comparing the average result with the certified values (Table S4). The sample results were corrected by the normalisation factor in order to be able to compare them with the results of reference samples. In the case of plant ash glasses, the average of normalization factors of standards B (mineral soda glass) and D (potash glass) was used for correcting the results. The pXRF results of the beads which contain <15 wt% PbO were corrected by averaging the calculated normalization factors for standard samples B (mineral soda glass) and C (lead glass). The lead oxide content of these beads lies between the measured amounts for standard samples B (0.48 wt%) and C (28.78 wt%).

Raman spectra of the samples were recorded by three instruments. The instruments included portable HE532 (Horiba Jobin Yvon, France) with a 532 nm Nd/YAG Ventus laser, HR Raman instrument (Horiba Jobin Yvon) with a 458 nm Ar-ion laser (Coherent) and T64000 micro-Raman spectrometer (HORIBA Jobin Yvon) with a 514.6 nm krypton-argon laser (Coherent). The details of the instruments, the procedures of the recording and processing of Raman spectra by correcting the baseline, are described elsewhere (Koleini et al., 2016b).

3. XRF and Raman results

3.1. The composition of glass

The beads were classified into six groups (Table 1) on the basis of their flux composition and silica source following Cagno et al. (2008). In this classification, the K_2O and CaO contents reflect the kind of flux used in the production of glass while the Al_2O_3 content gives information about the purity level of the silica source. The average amounts of seven major oxides measured by pXRF show that the majority of the beads are plant-ash silica glass with an average K_2O content of > 1.5 wt%. Five beads are outliers, with <1 wt% K_2O (c-739a, c-739e, c-739f, c-1835i, c-1843j). Fig. 2 displays CaO versus K_2O for the glass beads analysed which clearly shows different groups as follows: Group 1 (soda-lime plant-ash with 4 sub-groups), Group 2 (potash-rich with 2 sub-groups), Group 4 (mixed alkali) and Group 5 (mineral soda: outliers). The relative contents of Al_2O_3, CaO, K_2O and MgO are plotted in Fig. 3 which shows the same clusters of composition with some scattering due to the binary effects of Al_2O_3 and CaO on the composition. The contents of chlorine and lead oxide are

other criteria which add Groups 3 (synthetic soda) and 6 (lead soda) to the abovementioned list.

Table 1
As measured and corrected major and minor element oxide contents of glass beads presented in wt%

Groups	Sub-group		SiO_2	Al_2O_3	MgO	CaO	K_2O	Fe_2O_3	PbO	Balance
Group1 soda lime plant ash	hAl-hCa	Min	63.67	2.80	–	5.74	1.83	0.45	–	9.98
		Max	73.08	8.85	3.00	12.52	6.39	2.18	–	16.18
		Avg	67.89	4.21	1.38	8.80	4.75	0.89	–	12.07
		STD	2.14	1.39	0.71	1.58	1.01	0.34	–	1.14
	hAl-lCa	Min	65.20	3.70	–	2.84	2.43	0.19	–	9.23
		Max	74.88	9.73	2.24	5.63	3.79	3.89	–	15.32
		Avg	70.55	6.04	1.16	3.91	3.03	1.81	–	13.48
		STD	3.58	2.23	0.90	1.16	0.60	1.56	–	2.47
	lAl-hCa	Min	66.89	0.93	–	6.02	1.83	0.43	–	9.50
		Max	76.51	3.27	1.46	13.83	5.84	5.78	–	13.49
		Avg	70.40	2.17	0.85	8.75	4.12	1.76	–	11.96
		STD	2.35	0.51	0.49	1.90	1.32	1.64	–	1.11
	lAl-lCa	Min	67.90	1.53	–	2.14	1.80	0.23	–	10.88
		Max	76.61	2.73	2.29	5.93	5.41	5.03	–	15.79
		Avg	73.70	2.14	0.83	3.75	4.29	1.74	–	13.55
		STD	3.07	0.44	0.69	1.17	1.15	1.78	–	1.49
Group 2 Potash rich		Min	65.72	1.18	–	5.92	10.98	0.09	–	3.37
		Max	70.13	3.77	2.27	10.45	18.57	0.90	–	8.13
		Avg	68.35	2.31	1.20	7.22	14.30	0.18	–	6.43
		STD	1.29	0.81	0.86	1.21	1.90	0.18	–	1.21
Group 3 Synthetic soda		Min	70.01	2.34	–	5.06	2.02	0.36	–	13.97
		Max	74.75	4.23	1.19	7.37	3.55	0.57	–	15.46
		Avg	72.47	3.36	0.50	5.97	2.48	0.44	–	14.78
		STD	1.38	0.58	0.54	0.65	0.50	0.06	–	0.44
Group 4Mixed alkali		Min	66.97	1.04	–	6.11	7.81	0.04	–	11.47
		Max	71.14	3.90	0.97	8.51	9.48	0.94	–	13.06
		Avg	68.71	2.40	0.48	6.88	8.95	0.37	–	12.21
		STD	1.79	1.20	0.45	1.01	0.67	0.37	–	0.67
Group 5 Mineral soda		Min	71.43	1.54	–	5.18	0.90	0.39	–	11.50
		Max	75.67	2.45	0.93	9.99	1.33	0.93	–	19.31
		Avg	73.69	2.04	0.34	8.45	1.11	0.57	–	14.01
		STD	1.72	0.33	0.42	2.04	0.17	0.23	–	3.31
Group 6 Lead soda		Min	35.48	0.71	1.31	1.09	0.85	0.29	41.91	6.91
		Max	39.85	1.05	1.90	3.34	2.85	0.91	47.46	10.60
		Avg	37.48	0.82	1.56	2.37	2.00	0.68	43.96	8.95
		STD	1.95	0.16	0.26	0.94	0.90	0.27	2.46	1.71

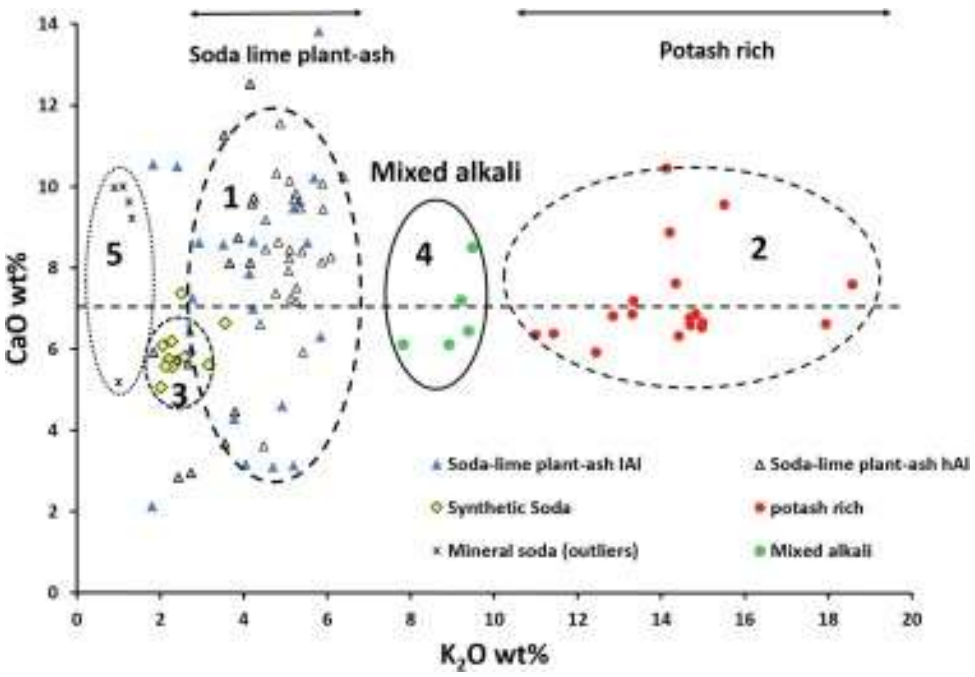

Fig. 2. Plot of CaO versus K_2O contents of European glass beads.

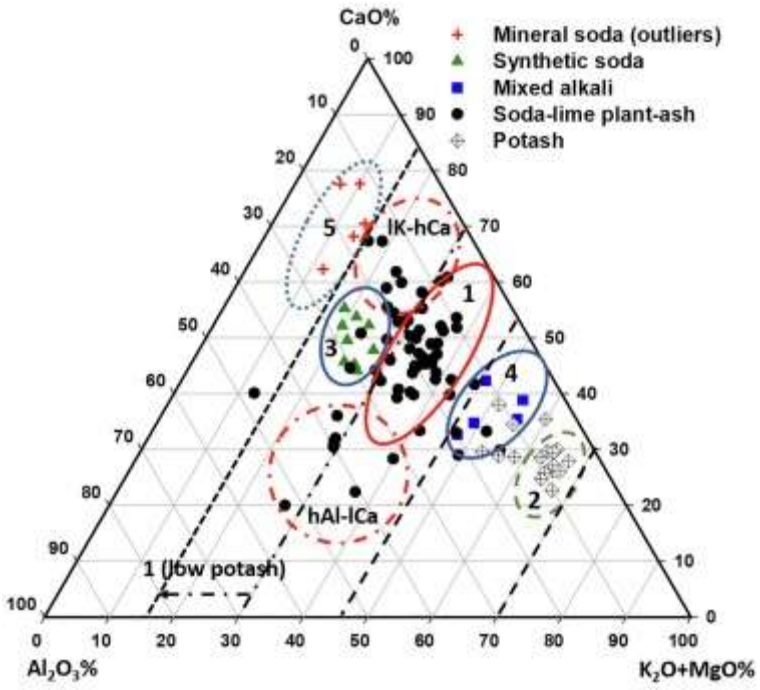

Fig. 3. Ternary diagram of CaO, Al_2O_3 and K_2O + MgO contents.

Position and intensity of the peaks in the Raman spectrum of an aluminosilicate glass are affected by the composition (Al/Si ratio, flux amount) and method of fabrication (melting temperature determining the nanostructure) (Colomban, 2003a). Thus, the differences in any of these criteria might modify the glass spectrum. The low covalence of Al-O bonds explains why the SiO_4 tetrahedron is the effective vibrational unit in establishing the relationship between spectral and structural characteristics (Colomban, 2003a, Labet and Colomban, 2013). All recorded spectra of the beads belonging to groups 1 to 5 show close positions of the Si-O bending and stretching peak maxima, however, some differences regarding components are observed (Fig. 4a). The Si-O bending peak maxima for these beads ranged from 537 to 570 cm^{-1} while the Si-O stretching peak maxima varied from 1092 to 1100 cm^{-1} which is characteristic of soda-lime glass. Table 2 shows a representative selection of the analysed beads in each group. The composition of each group is discussed as follows:

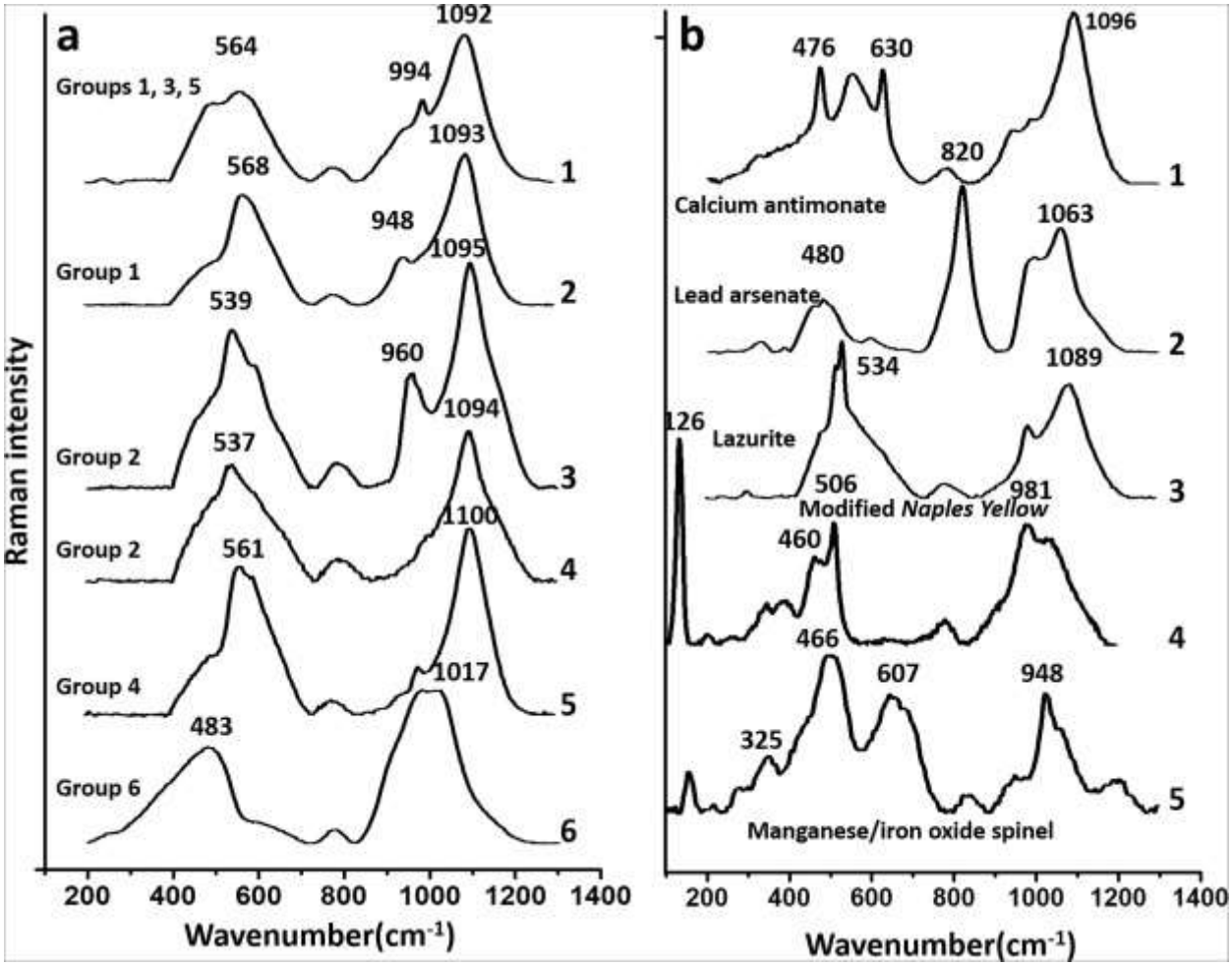

Fig. 4. Recorded Raman spectra of European glass beads coming from Southern Africa a) glass matrix, spectra acquired on soda lime glass with K_2O content < 4 wt% and synthetic soda (1); on soda lime glass with K_2O content > 5 wt% (2); on potash rich glass with high (3) and low phosphate contents (4); on mixed alkali glass (5); on lead soda glass (6); b) pigments and opacifiers.

Table 2
Dispersion of analysed beads by type, date and possible origins in selected sites. (The beads are kept in University of Pretoria museum. N. The number of beads.

Glass groups/types	Subgroups/bead%/Origin/date	Sites	Samples	N.
Group1Soda-lime plant-ash	High alumina + pure ash / (8%)Southern Europe15th-late 17th c.	Ml	62-73	2
		Mag	4-14-25	3
	High alumina + unrefined ash / (56%)Southern Europe15th-late 17th c.	Bd	14-24-25-26-27-44-152-163	8
		Ml		1
		Pr	56-90-93-102-82	5
		Map	112-116-117-124-130-132-140-142	8
		Mag	1-2-5-10	4
		D	1-4-6-7-9-11-12-13	8
	Low Al + pure ash / (11.5%)South and central Europe	Bd	120	1
		Ml	64-65	2
		Pr	51	1
		Map	122-123	2
		Mag	21-8	2
	Low Al + unrefined ash / (24.5%)South and central Europe	Bd	35-37	2
		Ml	63	1
		Pr	52-58-81-89-94-96-97	7
		Map	113-118-125-119	4
		Ba	6	1
Group 2Potash rich	High P_2O_5 (1.2–2.5 wt%) / (83%)BohemianLate 19th c.	Bd	30-31	1
		Pr	49	1
		Map	45	1
		Mag	30	1
		K2	1-2-3-4-32-33-42-43	8
	Low P_2O_5 (< 0.5 wt%) / (17%)Early 19th c.	K2	107-108-153	3
Groupe3Synthetic soda	K_2O < 4 wt%, mean Cl = 0.5Mean MgO = 0.5 wt%Late 19th-20th c.	Bd	5-6-7-8-158	5
		K2	9-11-12-28-29	5
Group 4Mixed alkali	19th c.	Bd	156	1
		Pr	47	1
		Mag	3-31-32	3
Group 5Mineral soda/	Natron/?	Bd	13-17-18	3
		PR	99-57	2
Group 6Lead soda	High lead oxide and low arsenatePbO > 40% and As_2O_3 < 6% wt%Late 17th c.	Pr	98	1
		Map	148-149	2
		K2	111	1
	Low lead oxide and high arsenatePbO < 37% and As_2O_3 > 9 wt%Early 19th c.	Bd	16-38-104-105-106-160-166-167-168-169	10
		Pr	83-85-86-91-92	5
		Ml	79	1
		Map	133-147-159	3
		K2	39-40-41-114	4
		Total		127

Note. Labels with underline show the beads with K2O < 3.5 wt%. Bd: Bambandyanalo, Ml: Maryland, Pr: Parma, Map: Mapungubwe, Mag:,Magoro Hill, D: Danamombe

3.1.1. Group 1 (Soda-lime plant ash glass)

The K_2O content of the beads vary between 1.8 and 6.4 wt% which is typical of the ashes used in the production of glass in the Mediterranean region, e.g. Levantine and Barilla ashes (Cagno et al., 2008, Cagno et al., 2012). The beads in this group were classified to four subgroups of high Al-high Ca, high Al-low Ca, low Al-high Ca and low Al-low Ca on the basis of Al_2O_3 and CaO content.

The CaO content displays a wide range from 2.1 to 13.8 wt% (Fig. 2, Fig. 3) as a result of different reasons. CaO content <4 wt% in glass might be due to the purification of soda ash or using plant ash with low lime content (Barkoudah and Henderson, 2006). The CaO content between 6 and 9 wt% shows the use of unrefined plant ash and the excess amount might be due to the addition of a calcium-rich raw material (Barkoudah and Henderson, 2006). The lime content of glass may also partially originate from the silica source (de Juan Ares and Schibille, 2017). Except for the twelve beads (Map122, 123, pr51, Ml62, 64, 65,73, Mag4, 14, 21, 25 and Bd120) with <4.6 wt% CaO content, the beads have a CaO content of >5.5 wt%, which indicates the use of unrefined soda ash in the production of the majority of the beads.

The majority of the beads (64%) in this group contain >3 wt% Al_2O_3, which is compatible with the high alumina soda-rich glass produced in the southern part of Europe except Venice during the Medieval and post-Medieval periods (Cagno et al., 2010, Cagno et al., 2012).

Soda-rich glass from the central and northern parts of Europe (*Façon-de-Venise*) usually contains low contents of Al_2O_3 (≤2 wt%) (De Raedt et al., 2002, Coutinho, 2016) (see Table S2). These high alumina beads were made of purified or unrefined ash (>6 wt% CaO) (see Fig. 3). Those beads (Ml62, 73, Mag4, 14, 25) made of refined ash (hAl-lCa) appeared in a separate area from samples made of unrefined ash in Fig. 3. This composition is very close to the beads of Mapungubwe series. Close compositions to abovementioned subgroups were reported for glass objects (*Façon-de-Venise*) which were found in Portugal (14th-17th centuries) and Italy (13th-16th centuries) (Cagno et al., 2010, Coutinho, 2016). The use of such purified ash in the production of glass only started during the second half of the 15th century in Venice (Coutinho, 2016).

Twenty-three samples (36%) with <2.5 wt% Al_2O_3 are consistent with the glass made from pure silica (likely quartz or flint pebbles). Low alumina glass was produced in a wider region, from the southern to northern parts of Europe. Fifteen of these samples were made of unrefined ash (lAl-hCa) (Fig. 1). Some of them with K_2O contents <3.5 wt% converge towards lK-hCa composition which is the case for the use of unrefined Levantine ash (Fig. 3). The zirconium and strontium contents of all low alumina beads in this group except Pr52, 58 and 94 are in accordance with the Venetian and Amsterdam glasses, with concentrations lower than 20 ppm and 400 ppm respectively (De Raedt et al., 2001). A mixture of pure silica and unrefined Levantine ash (>6 wt% CaO) was being used in the production of glass (*Vitrum Blanchum*) in Venice from the 11th century and later in Tuscan Italy (13th century) (Cagno et al., 2010, Verità and Zecchin, 2009). Similar compositions were also reported for glass samples (*Façon-de-Venise*) found in Portugal, Spain, Antwerp, Amsterdam and London dated to the 16th and 17th century CE (De Raedt et al., 2001, Coutinho, 2016, Dussubieux and Karklins, 2016, Ulitzka, 1994). Only eight samples of this subgroup (see Table 2) were made of pure ash (<6 wt% CaO) and siliceous pebble (lAl-lCa) (Fig. 2). These beads contain higher alumina than the common Venetian *Cristallo* (0.68 ± 0.14 wt%) as reported by Verità and Zecchin (2009). Close compositions to these subgroups have also been reported from the 17th century productions of Antwerp (De Raedt et al., 2002), London, Amsterdam (Dussubieux and Karklins, 2016) and Coimbra (Coutinho, 2016).

Raman analyses show two different types of glasses for the beads classified in Group 1. The beads with low K_2O content (<4 wt%) show the typical spectrum 1 (Fig. 4a). Spectrum 2 represents the Raman signature of those beads with K_2O content of >5 wt%. The spectrum shows a broad peak at 948 cm^{-1} which makes it different from the spectrum of the beads with lower K_2O content. Fukumi et al. (1990) mention that the type and amount of the alkali have a direct effect on the intensity of the peak at 950 cm^{-1} in the silicate glass. They showed that the alkalis with higher atomic number as in the case of potassium would increase the peak intensity at 950 cm^{-1} more than the lower atomic number alkalis such as soda. These beads were produced with western Mediterranean ash with high K_2O content as compared to Levantine ash.

3.1.2. Group 2 (potash-rich glass)

All the 18 beads in this group are hexagonal and cobalt blue except one annular bead (K2-153) (Fig. 1). Two hexagonal beads (K2-107, 108) are simple while the rest of the beads are compound in structure. The simple and the compound hexagonal beads are in accordance with Karklins (1985a) 'If5′ and 'IIIf2′ types respectively. The K_2O content of the beads is between 10.9 and 18.6 wt%. The CaO content varies between 5.9 and 10.5 wt% (Fig. 2, Fig.

3). Simple and compound hexagonal beads show differences in phosphate content, which places them in two subgroups with high and low phosphate content.

The majority of the beads except the simple hexagonal beads (If5) and one annular bead (K2-107, 108, 153), contain high P_2O_5 (1.2–2.5 wt%) which is characteristic of wood ash alkali (Table S5). The K_2O/CaO ratio of the samples is between 1.3 and 2.7 which makes them close to potash-rich glass, introduced as K-Ca-3 glass by Stern and Gerber (2004). According to these authors, K-Ca-3 glass was manufactured by the addition of a potash-rich material (extracted potash) to the leached vegetable ash and silica source. Extracted potash is produced by leaching of the fresh wood ash, and is poor in insoluble oxides like lime, magnesia, phosphate, iron and manganese as such (Stern and Gerber, 2004). However, leached ash contains insoluble minerals of wood ash which could be the most probable source of phosphate and lime in this type of glass (Cílová and Woitsch, 2012, Stern and Gerber, 2004). Bone ash is another alternative source of phosphate and calcium in this type of glass as reported by Costa et al. (2019).

In the case of samples with phosphate content lower than 0.5 wt% (K2-107, 108, 153), the leached ash had been probably replaced by a mineral source of calcium such as limestone (potash-lime glass) (Stern and Gerber, 2004). The latter beads also contain MnO_2 (0.4–3.3 wt%) which is reported as a substance used for the production of ordinary colourless glass, a mixture of sand, lime and potash ash, in Central Europe in the beginning of the 18th century (Coutinho, 2016, Kunicki-Goldfinger et al., 2005).

However, the source of calcium (leached ash or a natural mineral) divides them further into two subgroups as also demonstrated by Raman spectra 3 and 4 (Fig. 4a). The spectra show that the Si-O bending peak maxima were observed in a lower wavenumber region (535–540 cm^{-1}) compared to the beads in Group 1. Spectrum 3 is related to potash-rich glass with high phosphate content. The strong peak at 960 cm^{-1} is the signature of calcium phosphate crystalline precipitates (Ricciardi, et al., 2009). The same spectra were reported for some hexagonal beads and one annular bead from Congo (Rousaki et al., 2016) and one Mapungubwe hexagonal bead (Tournié et al., 2012). Accordingly, the peak at 960 cm^{-1} is not observed in potash-rich beads with low phosphate content (spectrum 4).

3.1.3. Group 3 (Synthetic soda glass)

All the beads in this group are annular and have dark blue colour. They contain K_2O in the range of 2–3.6 wt% and CaO in the range of 5–7.4 wt%. These beads have lower contents of MgO (mean value = 0.5 wt%) and chlorine (mean value = 0.3 wt%) in comparison with the beads in Group 1 with low K_2O content (see Tables 1 and S5). Low content of chlorine indicates that the alkali has a mineral synthetic source although the potassium content of the samples is higher than that of usual synthetic soda glass with < 0.5 wt% K_2O in the composition (Dungworth, 2011). These samples have a close composition with the annular beads found at Fichtelgebirge and Mehlmeisel, Germany, dated to the late 19th and the early 20th century (Karklins et al., 2016). It was indicated that the high amounts of K_2O (2.2–5.7 wt%) in the annular beads of Fichtelgebirge is probably due to the presence of feldspar in the sand. This might be also due to the addition of saltpetre (potassium nitrate) which was in use as a refining agent from the 1870 s onwards (Dungworth, 2011).

The Raman spectrum of these beads is the same as the beads in Group 1 with low potassium content (<4 wt% K_2O) (Fig. 4a, spectrum 1).

3.1.4. Group 4 (Mixed alkali glass)

Only five beads belong to this group. Except one light blue drawn bead, the rest are hexagonal and annular beads. The samples in this group have a K_2O content between 7.8 and 9.5 wt%, which is high for common soda-rich glasses with typically <5 wt% K_2O content (Dungworth et al., 2006). In the same way, the K_2O content is lower than in common potash-rich glass with >10 wt% in composition (Coutinho, 2016). The amount of CaO varied between 6 and 8.5 wt%. These values are too low for a high lime low alkali glass. Fig. 2, Fig. 3 show that these samples have a composition between potash-rich glass (forest and wood ash glass) and plant ash soda-lime glasses as mentioned by Dungworth and Mortimer, 2005, Coutinho, 2016. It was reported that low quality or purification of the consumed plant ash might be the reason behind the formation of these mixed alkali glasses (Dungworth et al., 2006, Tite et al., 2006).

All the beads in this group except the annular bead (Mag32) contain <0.6 wt% phosphate (Table S5). Therefore, it is possible that the hexagonal beads had been produced by adding a higher amount of soda (soda culet) to potash-rich glass with low phosphate content in Group 2. The annular bead (Mag32) contains 1 wt% phosphate, indicating the use of wood ash as part of the alkalis used in its production. Spectrum 5 in Fig. 4a was recorded on mixed alkali glass (Group 4) with the glass signature similar to the beads with the same morphology (type 6: If5) from Kongo Kingdom (Coccato et al., 2017).

3.1.5. Group 5 (Outliers)

This group consists of five beads with <1.1 wt% K_2O and high chlorine content (mean value = 1.2 wt%) (Tables 1 and S5). The low alumina content (<2.5 wt%) indicates the use of pebble as the source of silica. CaO content is high with the mean value of 8.45 wt%. Four white beads contain lead oxide (mean value = 8.5 wt%) which discriminates them from the only cobalt blue bead (Pr99) in this cluster. The composition of these beads is compatible with mineral soda glass (natron) produced from the Roman times until the early medieval period in Europe (Verità, 2013). However, the presence of natron glass does not coincide chronologically with the archaeological context where the beads were found. On the other hand, the high chlorine content shows that the beads could not have been made with synthetic soda. The Raman spectrum of these beads is the same as the beads in Group 1 with low K_2O content as well as the ones in Group 3 (synthetic soda glass) (Fig. 4a, spectrum 1).

3.1.6. Group 6 (lead-soda glass)

Among the analysed beads, 28 samples contain high levels of lead (Table 1). The majority of these beads (24 samples) also contain elevated amounts of arsenate (>9 wt%), indicating that these beads were opacified with lead arsenate. Lead arsenate beads consist of some simple beads in white, pink, pale light blue. White hearth and striped beads which are compound in the structure (the beads are made of two different coloured layers) are found in this group as well (Fig. 1). Due to the lack of a standard sample with close composition to these beads, their compositions were reported as measured by pXRF in Table S5.

Four green beads (K2-111, Pr98, Map148-149) contain high amounts of lead oxide above 40 wt% and low amounts of arsenate less than < 6 wt% which discriminates these beads from those mentioned above (Table 1). These beads were opacified with calcium antimonate

($Ca_2Sb_2O_7$) (Table S5). Previous Raman spectroscopy analysis placed both categories of lead glasses as lead-soda glass (Koleini et al., 2016a, Tournié et al., 2012).

Raman spectrum 6 (Fig. 4a) is related to the beads with high lead content. After the baseline subtraction procedure eliminating the strong Boson peak below 300 cm^{-1}, the Si-O bending and stretching peak maxima were observed from 450 to 500 cm^{-1} and 949 to 1060 cm^{-1} respectively (Tournié et al., 2012). No lead arsenate phase was observed in the beads with low arsenate content.

3.2. Pigments and opacifiers

Fig. 4b shows the spectra with the significant contribution of pigments and opacifiers in the beads. Pigments identified are listed in Table S6. Calcium antimonate ($Ca_2Sb_2O_7$) with two strong peaks at 480 cm^{-1} and 630 cm^{-1} was detected as an opacifier in some of the beads in groups 1, 5 and 6 (spectrum 1). Calcium antimonate has been in use since antiquity. However, it was the predominant opacifier from the middle of the 17th to 19th centuries in Europe (Hancock et al., 1997). The presence of antimonates in soda- rich plant ash glass (Group 1) shows that the samples are dated to the times of the decline of Venetian glass and the spread of *Façon de Venise* in Europe during the mid-17th century (Coutinho, 2016, Verità, 2013).

Arsenate-based phases are characterized with a strong peak at around 815–830 cm^{-1}, as detected in lead-soda glass of Group 6 (spectrum 2, Fig. 4b) (Colomban et al., 2018). Lead arsenate was in use from the 16th century onwards in the production of *lattimo* glass in Venice (Ricciardi, et al., 2009). Due to its toxicity, predominant use only started in the 19th century and continued into the 20th century (Kirmizi et al., 2010, Bonneau et al., 2013). Therefore, all the beads including lead arsenate are attributed from the early 19th to the 20th centuries.

Ultramarine (synthetic mineral) or lapis lazuli (natural rock with the blue mineral lazurite) was detected in three light blue beads (Bd120, Map122 and Mag25) (spectrum 3, Fig. 4b) with the characteristic sharp peak of S-S bond chromophore at ~ 540 cm^{-1} which is hosted in zeolite (synthetic) or feldspar (natural) framework (Koleini et al., 2016a, Tournié et al., 2012). The beads also contain antimony and copper ions as the opacifier and the blue colorant respectively (Table S5). Swirls of different shades of blue are visible on the surface of these three oblate-shaped beads, indicating that the chromophore did not distribute evenly in the glass matrix, according to the dispersion of pigments. The beads have different glass compositions due to their alumina (Map122 and Mag25) or K_2O content (Bd120) (Table S5).

The natural mineral (lazurite) was in use since antiquity (Edwards et al., 2004) and artificial ultramarine was being produced during the early 19th century. The natural lazurite is found in the Islamic glazes and enamels from Iran (13th-14th century), the Mamluk Sultanate (13th-15th centuries) and Italy (13th century) (Colomban, 2003b, Caggiani et al., 2013). Natural lazurite was probably used for colouring the beads since the beads fall in soda-rich alkali group (Group 1). Their production began to decline in the 18th century when artificial ultramarine had not been produced yet (Coutinho, 2016). Tournié et al. (2012) attributed these beads to production in Fustat and Iran, although it is possible that the beads were produced in southern Europe where the glass industry had been influenced by traditional Islamic glass recipes until the 15th century (Verità, 2013).

Modified *Naples Yellow* (Pb-Sn-Sb triple oxides, $Pb_2Sb_{2-x-y}Sn_xM_yO_{7-\delta}$) with peaks at 125 to 135 cm^{-1} (Pb^{2+} ion mode), 458 cm^{-1} (Sn-O mode) and 507 cm^{-1} (Sb-O mode) (Rosi et al., 2009) was detected in three green beads in Group 6 (spectrum 4, Fig. 4b). This pigment was also in use since antiquity. However, antimony found in southern Africa yellow and green beads was only detected in European beads (Koleini et al., 2016a, Tournié et al., 2012).

Manganese/iron oxide spinel with typical strong peaks around 470 cm^{-1} and 600–640 cm^{-1} (Spectrum 5) was detected in four black beads (Mag1, Ml62, 65 and 73) in Group 1 (Koleini et al., 2016a, Tournié et al., 2012). These beads have a high manganese oxide content (mean value = 16.87 wt%). Black beads with manganese oxide were also reported from Kindoki in Congo and Mbanza Kongo in Angola (Costa et al., 2019, Rousaki et al., 2016). Manganese oxide as a black pigment was in use since antiquity in eastern Anatolia and later spread out towards the southern Balkans and northern Italy (Noll, 1979, Schweizer and Rinuy, 1982). Mn-rich spinel was reported as a black pigment in the glazed pottery fragments and glass from the 13th to 16th centuries in Italy (Clark et al., 1997). Three of the black beads contain a low amount of lead oxide (7–10 wt%) which makes them different from Mag1.

A low amount of lead oxide (2.5–13 wt%) was also detected in some of the white, light blue and brownish-red beads in groups 1 and 5 (Table S5). These beads are coloured or opacified with calcium antimonate ($Ca_2Sb_2O_7$) or contain cuprous oxide in the case of brownish-red beads. This low amount of lead shows a slight downward shift of Si-O stretching peak maxima in some of these beads. Sayre and Smith (1967) reported that the addition of lead in glass increases the solubility of copper, antimony and tin oxides at high temperatures that may lead to glass opacification by precipitation of oxide particles at lower temperatures. This method was in practice for the production of brownish-red glass coloured with copper nanoparticles since antiquity (Henderson, 1985, Freestone, 1987) and continued in Islamic glass production (Mecking, 2013) and later in post-medieval Europe (Dussubieux and Karklins, 2016). The opacification of glass with antimony in the presence of lead was practiced during the Roman times (Lahlil et al., 2010). In the case of antimony, lead content between 4 wt% and 25 wt% facilitates the formation of $Ca_2Sb_2O_7$ instead of $CaSb_2O_6$ in the glass (Lahlil et al., 2010). As a result, the brownish-red, black and antimonate-opacified beads were found to be manufactured using two different methods, with or without the addition of lead oxide in the composition. This indicates the possible different origins of the beads.

4. Discussion

We identified six different glass compositions regarding the imported European beads to southern Africa (Table 1). The glass beads in Group 1 are soda-lime plant ash type and were produced using Levantine or West Mediterranean ashes. These could be the earliest European beads to have been imported into southern Africa from the early 16th century onwards. However, the majority of the beads in this group contains calcium antimonate ($Ca_2Sb_2O_7$) which shows that the beads predominantly belong to the second half of the 17th century. This date coincides with the arrival of Dutch and English traders in southern Africa (Theal, 1902, Smith, 1970). There are only eight beads with no antimony content in the case of black, brownish red on black, plum, light and dark blue colours. Big differences in CaO and Al_2O_3 contents of the beads in Group 1 are consistent with the productions of different workshops/factories. Both high and low alumina glass beads are found in Group 1. While soda-glass with high alumina content is confined to southern Europe, the low alumina glass has been produced in a wider region from South into Central Europe (see Table S2). The

contents of Sr and Zr in low alumina beads show that the composition of some of the beads are close to those of the glass productions in Amsterdam and Venice. The amount of alumina in these beads is however not in the range of Venetian beads. Therefore, a more detailed study is required to identify the production places of the low alumina beads in Europe. The composition of European high alumina glass produced by purified plant ash is close to that of the Mapungubwe series imported to southern Africa from 1240 to 1300 CE. Morphology and the kind of opacifier which is calcium antimonate ($Ca_2Sb_2O_7$) in European beads constitute the differences of these two series.

The beads analysed here have black, dark and light blue, plum colours as well as brownish-red on black and green or blue on light grey colours in the case of a series of compound beads. Francis, 1998, Karklins, 1985b reported that compound brownish-red beads were produced in Venice and Amsterdam respectively during the late 16th century. All of the compound beads in this assemblage, except Map123, contain calcium antimonate ($Ca_2Sb_2O_7$) which allows attributing them to the second half of the 17th century. The date is in accordance with that of Beck who mentioned that these beads were brought into southern Africa from the 18th to the 19th century (Caton-Thompson, 1931).

Hexagonal beads have been common in southern Africa since the early 19th century (Francis, 1994, Van der Sleen, 1967, Wood, 2008). The beads have compound or simple structure and different sizes. Venice was mentioned as a production centre (DeCorse et al., 2003, Wood, 2008). Francis (1979) reported that these beads were also produced in Bohemia (now Czech Republic). The compound beads (dark blue on white) are known as *Ambassador* beads and were produced in both Venice and Bohemia (Francis, 1979). The morphology of compound beads in this assemblage is similar to that of Bohemian beads reported in Francis (1979) dated to the late 19th century. All the compound hexagonal beads are potassium-rich glass with high phosphate content (Group 2). Although similar glass composition with high potash-high phosphate beads has been reported for cobalt blue annular beads from Fichtelgebirge in Bavaria (Karklins et al., 2016), compound hexagonal beads were not present in this collection.

Simple hexagonal beads (small and large) are among low phosphate beads in Group 2 or mixed alkali glass in Group 4. A small imported hexagonal bead with the same composition as the low phosphate beads in Group 2 was reported from North America, dated to the early 19th century (Karklins et al., 2016). This composition is attributed to the glass production of Central Europe from the 18th century (Coutinho, 2016, Kunicki-Goldfinger et al., 2005) to the 19th century (Karklins et al., 2016). The differences in the phosphate content of Group 2 beads are due to the different sources of lime used in the beads. The mixed alkali beads seem to have been produced by the addition of soda culet to the potash-low phosphate glass. Therefore, the hexagonal beads were produced with the use of three recipes and may be of three separate origins.

Annular beads have three different compositions although the majority of them are made of synthetic soda (Group 3). Two annular beads, K2-153 and Mag32, were placed in potash-rich glass with low phosphate content (Group 2) and mixed alkali glass (Group 4) respectively. Different compositions indicate that the beads were manufactured in three different places. K2-153 has the same composition with that of the small hexagonal beads (K2-107 and 108) with low phosphate content and it is probably of the same origin. The same composition was reported for amber-coloured annular beads found at Fichtelgebirge (Karklins et al., 2016). The cobalt blue beads were probably imported together with amber-coloured annular beads to

southern Africa during the early 19th century (Francis, 1993). It should be mentioned that potash glass had been in production until the mid-19th century in England. The annular beads made of synthetic soda might be later in date because the synthetic soda was used in the production of glass (first Leblanc and then, Solvay soda glass) from 1830 onwards in Europe (Dungworth, 2011). This later composition is probably related to cobalt blue annular beads which Francis (1993) referred to in terms of their importation to southern Africa during the late 19th century.

The mixed alkali beads with the same morphology as the simple hexagonal and annular beads in Groups 2 and 3 respectively are also similar in P_2O_5 and chlorine contents. Low phosphate content of simple hexagonal beads shows that they were probably made by the addition of excess amount of other alkali such as soda or limestone to the potash-rich glass. Hexagonal and annular beads with mixed alkali composition were also reported from archaeological sites in Congo in Central Africa (Rousaki et al., 2016).

Although it is clear that the mineral soda beads in Group 5 were made by natron as alkali, dating of the beads remains problematic. Here, calcium antimonate ($Ca_2Sb_2O_7$) in the white beads cannot be used as a chronological marker since the pigment was in use during the Roman times as well. On the other hand, the beads were found along with later European beads in the same context in Parma Farm and Bambandyanalo in southern Africa. It is possible these beads were made from recycling earlier glass probably dating to the medieval period in Europe.

The lead-soda glass (Group 6) shows two different compositions. Some of these beads were opacified with arsenate. These beads were being produced during the 19th and the 20th centuries. The second part of beads was opacified with calcium antimonate, which allows attributing them to a period from the late 17th to the late 19th century. The latter are close in terms of morphology and composition to drawn green beads found in Garumele, in West African Niger (Robertshaw et al., 2014).

5. Conclusion

Raman and pXRF as two non-destructive and mobile methods are significantly effective in detecting different types of glass represented in this paper. We identified six different glass compositions for the imported European beads to southern Africa and proposed some provenances. The results show that Raman analysis can detect soda-lime, potash and lead-soda glass by recording a single spectrum. Although Raman analysis can differentiate between low and high K_2O content soda-lime glass, it cannot discriminate synthetic soda, natron and mixed alkali types from them. pXRF could fill this gap by the semi-quantitative measuring of elements. The detection of pigments and opacifiers in glass by Raman analysis sheds a new light for dating the beads.

6. Author statement

Conception and design of study: Farahnaz Koleini and Philippe Colomban

Acquisition of data: Farahnaz Koleini, Philippe Colomban and Innocent Pikirayi

Analysis and/or interpretation of data: Farahnaz Koleini and Philippe Colomban

Drafting the manuscript: Farahnaz Koleini

Revising the manuscript critically for important intellectual content: Philippe Colomban

Supervision: Innocent Pikirayi

Approval of the version of the manuscript to be published: Farahnaz Koleini, Philippe Colomban and Innocent Pikirayi

Acknowledgments

The authors would like to thank University of Pretoria Museum for the glass beads used in the analyses and Stephen P. Koob and Corning Museum of glass for supplying the standard glass samples and Dr Burcu Kirmizi for editing the text. Farahnaz Koleini and Innocent Pikirayi acknowledge the financial contribution from the South African National Research Foundation (NRF) Competitive Program for Rated Researchers (CPRR) project titled Great Zimbabwe's Complexity (2017-2019) grant no. 105866.

References

Barkoudah, Y., Henderson, J., 2006. Plant ashes from Syria and the manufacture of ancient glass: ethnographic and scientific aspects. J. Glass Stud. 48, 297–321.

Bonneau, A., Moreau, J., Auger, R., Hancock, R.G.V., Émard, B., 2013. Analyses physico-chimiques
des perles de traite en verre de facture européenne: quelles instrumentations pour quels résultats? Archéologiques 26, 109–132.

Caggiani, M.C., Colomban, Ph., Valotteau, C., Mangone, A., Cambon, P., 2013. Mobile Raman spectroscopy analysis of ancient enamelled glass masterpieces. Anal. Methods 5, 4345–4354.

Cagno, S., Brondi Badano, M., Mathis, F., Strivay, D., Janssen, K., 2012. Study of medieval glass from Savona (Italy) and their relation with the glass produced in Altare. J. Archaeol. Sci. 39, 2191–2197.

Cagno, S., Janssens, K., Mendera, M., 2008. Compositional analysis of Tuscan glass samples: in search of raw material fingerprints. Anal. BioAnal. Chem. 391, 1389–1395.

Cagno, S., Mendera, M., Jeffries, T., Janssens, K., 2010. Raw materials for medieval to post-medieval Tuscan glassmaking: new insight from LA-ICP-MS analyses. J. Archaeol. Sci. 37, 3030–3036.

Caton-Thompson, G., 1931. The Zimbabwe Culture. Clarendon Press, Oxford.

Cílová, Z., Woitsch, J., 2012. Potash e a key raw material of glass batch for Bohemian glasses from 14 the17th centuries? J. Archaeol. Sci. 39, 371–380.

Clark, R.J.H., Curri, L., Henshaw, G.S., 1997. Characterization of brown-black and blue pigments in glazed pottery fragments from Castel Fiorentino (Foggia, Italy) by Raman microscopy, X-ray photoelectron spectroscopy. J. Raman Spectrosc. 28, 105–109.

Costa, M., Barrulas, P., Dias, L., da Conceição Lopes, M., Barreira, J., Clist, B., Karklins, K.,

da Piedade de Jesus, M., da Silva Domingos, S., Vandenabeele, P., Mirão J., 2019. Multi-analytical approach to the study of the European glass beads found in the tombs of Kulumbimbi (Mbanza Kongo, Angola), Microchem. J. 149, 103990.
Coccato, A., Costa, M., Rousaki, A., Clist, B., Karklins, K., Bostoen, K., Manhita, A., Cardoso, A., Barrocas Dias, C., Candeias, A., Moens, L., Mirão, J., Vandenabeele, P., 2017. Micro-Raman spectroscopy and complementary techniques (hXRF, VP-SEMEDS, μ-FTIR, Py-GC/MS) applied to the study of beads from the Kongo Kingdom (Democratic Republic of the Congo). J. Raman Spectrosc. 48, 1468–1478.

Colomban, Ph., 2003a. Polymerization degree and Raman identification of ancient glasses used for jewelry, ceramic enamels and mosaics. J. Non-Cryst. Solids 323, 180–187.

Colomban, Ph., 2003b. Lapis lazuli as unexpected blue pigment in Iranian Lâjvardina ceramics. J. Raman Spectrosc. 34, 420–423.

Colomban, Ph., Maggetti, M., d'Albis, A., 2018. Non-invasive Raman identification of crystalline and glassy phases in a 1781 Sèvres Royal Factory soft paste porcelain plate. J. Eur. Ceram. Soc. 38, 5228–5233.

Coutinho, I., 2016. New insights into 17th and 18th century glass from Portugal: Study and Preservation. Dissertation, Universidade Nova de Lisboa.

Craig, N., Speakman, R.J., Popelka-Filcoff, R.S., Glascock, M.D., Robertson, J.D., Shackley, M.S., Aldenderfer, M.S., 2007. Comparison of XRF and PXRF for analysis of archaeological obsidian from southern Perú. J. Archaeol. Sci. 34, 2012–2024.

DeCorse, C.R., Thiaw, F.G., Thiaw, I., 2003. Toward a systematic bead description system: a view from the Lower Falemme, Senegal. J. Afr. Archaeol. 1, 77–110.

de Juan Ares, J., Schibille, N., 2017. Glass import and production in Hispania during the early medieval period: The glass from Ciudad de Vascos (Toledo). PLoS One. 12, e0182129. https://doi.org/10.1371/journal.pone.0182129.

De Raedt, I., Janssens, K., Veeckman, J., 2002. On the distinction between 16th and 17th century Venetian and Façon-de-Venise glass. In: Veeckman, J. (Ed.), Majolica and Glass: from Italy to Antwerp and Beyond. The Transfer of Technology in the 16th - early 17th Century. Stad Antwerpen, Antwerp, pp. 95–121.

De Raedt, I., Janssens, K., Veeckman, J., Vincze, L., Vekemans, B., Jeffries, T.E., 2001. Trace analysis for distinguishing between Venetian and Façon-de-Venise glass vessels of the 16th and 17th century. J. Anal. At. Spectrom. 16, 1012–1017.

Dungworth, D., 2011. The value of historic window glass. Hist. Environ. Policy Pract. 2, 21–48. https://doi.org/10.1179/175675011X12943261434567.

Dungworth, D., Cromwell, T., Ashurst, D., Cumberpatch, C., Higgins, D., Willmott, H., 2006. Glass and pottery manufacture at Silkstone, Yorkshire. Post-Medieval Archaeol. 40, 160–190.

Dungworth, D., Mortimer, C., 2005. Examination of Glassworking Materials from Cheese Lane, Bristol, Centre for Archaeology Report Series, English Heritage, no. 6/2005. ISSN 1473-9224.

Dussubieux, L., Karklins, K., 2016. Glass bead production in Europe during the 17th century: elemental analysis of glass material found in London and Amsterdam. J. Archaeol. Sci. Rep. 5, 574–589.

Edwards, H.G.M., Villar, E.S.J., Eremin, K.A., 2004. Raman spectroscopic analysis of pigments from dynastic Egyptian funerary artefacts. J. Raman Spectrosc. 35, 786–795.

Fouché, L., 1937. Mapungubwe. University Press, Cambridge.

Francis Jr., P., 1979. The Czech Bead Story, World of Beads Monograph Series 2. Lapis route book, New York.

Francis Jr., P., 1993. Advanced bead identification. The Center for Bead Research Lake Placid, NY.

Francis Jr., P., 1994. Beads of the World. Schiffer Publishing Ltd, Atglen, PA.

Francis Jr., P., 1998. The Venetian Bead Story, part 1: history. Margaretologist 11, 3–12.

Freestone, I.C., 1987. Composition and Microstructure of Early Opaque Red Glass. In: Bimson, M., Freestone, I. (Eds), Early Vitreous Materials, British Museum occasional paper 56, pp. 173-191.

Freestone, I.C., Gorin-Rosen, Y., Hughes, M.J., 2000. Composition of primary glass from Israel. In: Nenna, M.D. (Ed.), Ateliers primaires et secondaires de verriers du second millénaire av. J.-C. au Moyen-Age, Travaux de la Maison de l'Orient Méditerranéen no. 33, Lyon, pp. 65-84.

Fukumi, K., Hayakawa, J., Komiyama, T., 1990. Intensity of Raman band in silicate glasses. J. Non-Cryst. Solids 119, 297–302.

Gratuze, B., 2013. Provenance analysis of glass artefacts. In: Janssens, K. (Ed.), Modern methods for analysing archaeological and historical glass. John Wiley and Sons, Chichester, UK, pp. 311–340 Available at: http://onlinelibrary.wiley.com/book/10.1002/9781118314234.

Hancock, R.G.V., Aufreiter, S., Kenyon I., 1997. European white glass trade beads as chronological and trade markers. In: Vandiver, P., Druzik, J.R., Merkel, J.F., Stewart J. (Eds.), Materials Issues in Art and Archaeology V, Materials Research Society Symposium Proceedings, vol. 462. Materials Research Society, Pittsburgh, PA, pp. 181-191.

Henderson, J., 1985. The raw material of early glass production, Oxford. J. Archaeol. 4, 267–291.

Huffman, T., 2000. Mapungubwe and the origins of the Zimbabwe culture, S. Afr. Archaeol. Soc. Goodwin Ser. 8, 14–29.

Karklins, K., 1985a. Glass Beads: The Levin Catalogue of Mid-19th Century Beads: A Sample Book of 19th Century Venetian beads: Guide to the Description and Classification of Glass Beads. Parcs Canada, Ottawa.
Karklins, K., 1985b. Early Amsterdam trade beads. Ornament 9, 36–41.

Karklins, K., Jargstorf, S., Zeh, G., Dussubieux, L., 2016. The Fichtelgebirge bead and button industry of Bavaria. J. Soc. Bead Res. 28, 16–37.

Kirmizi, B., Colomban, Ph., Blanc, M., 2010. On-site analysis of Limoges enamels from sixteenth to nineteenth centuries: an attempt to differentiate between genuine artefacts and copies. J. Raman Spectrosc. 41, 1240–1247.

Koleini, F., Colomban, Ph., Pikirayi, I., Prinsloo, L.C., 2019a. Glass beads, markers of ancient trade in sub-Saharan Africa: methodology, state of the art and perspectives. Heritage 2, 2343–2369.

Koleini, F., Machiridza, L.H., Pikirayi, I., Colomban, Ph., 2019b. The chronology of Insiza cluster Khami-phase sites in south-western Zimbabwe: compositional insights from pXRF and Raman analysis of excavated exotic glass finds. Archaeometry 61, 874–890. https://doi.org/10.1111/arcm.12463.

Koleini, F., Pikirayi, I., Colomban, Ph., 2017. Revisiting Baranda: a multi-analytical approach in classifying sixteenth/seventeenth-century glass beads from northern Zimbabwe. Antiquity 91, 751–764.

Koleini, F., Prinsloo, L.C., Biemond, W.M., Colomban, Ph., Ngo, A.T., Boeyens, J., van der Ryst, M., van Brakel, K., 2016a. Unravelling the glass trade bead sequence from Magoro Hill, South Africa: separating pre-17th-century Asian imports from later European counterparts. Heritage Sci. 4, 43.

Koleini, F., Prinsloo, L.C., Biemond, W.M., Colomban, Ph., Nego, A., Boeyens, J., van der Ryst, M., 2016b. Towards refining the classification of glass trade beads imported into southern Africa from the 8th to the 16th century AD. J. Cult. Heritage 19, 435–444.

Kunicki-Goldfinger, J.J., Kierzek, J., Dzierzanowski, P., Kasprzak, A., 2005. Central European crystal glass of the girst half of the 18th century. In: Annales du 16th Congrès de l'Association Internationale pour l'Histoire du Verre (AIHV), 7th to 13th September 2003. Nottingham, London, pp. 258–262.

Labet, V., Colomban, Ph., 2013. Vibrational properties of silicates: A cluster model able to reproduce the effect of "SiO4" polymerization on Raman intensities. J. Non-Cryst. Solids 370, 10–17.

Lahlil, S., Biron, I., Cotte, M., Susini, J., 2010. New insight on the in situ crystallization of calcium antimonite opacified glass during the Roman period. Appl. Phys. A 100, 683–692.

Mecking, O., 2013. Medieval lead glass in central Europe. Archaeometry 55, 640–662.

Noll, W., 1979. Anorganische Pigmente in der Vorgeschichte und Antike. Fortschr Miner 57, 203–263.

Peinado, F.M., Ruano, S.M., González, M.G.B., Molina, C.E., 2010. A rapid field procedure for screening trace elements in polluted soil using portable X-ray fluorescence (PXRF). Geoderma 159, 76–82. https://doi.org/10.1016/j.geoderma.2010.06.019.

Prinsloo, L.C., Tournié, A., Colomban, Ph., 2011. A Raman spectroscopic study of glass trade beads excavated at Mapungubwe hill and K2, two archaeological sites in southern Africa, raises questions about the last occupation date of the hill. J. Archaeol. Sci. 38, 3264–3277.

Ricciardi, P., Colomban, Ph., Tournie, A., Milande, V., 2009. Non-destructive on-site identification of ancient glasses: genuine artefacts, embellished pieces or forgeries? J. Raman Spectrosc. 40, 604–617.

Robertshaw, P., Wood, M., Haour, A., Karklins, K., Neff, H., 2014. Chemical analysis, Chronology, and context of a European glass bead assemblage from Garumele, Niger. J. Archaeol. Sci. 4, 591–604.

Rosi, F., Manuali, V., Miliani, C., Brunetti, B.G., Sgamelloti, A., Grygar, T., Hradil, D., 2009. Raman scattering features of lead pyroantimonate compounds. Pat I: XRD and Raman characterization of Pb2Sb2O7 doped with tin and zinc. J. Raman Spectrosc. 40, 107–111.

Rostron, P.D., Ramsey, M.H., 2017. Quantifying Heterogeneity of Small Test Portion Masses of Geological Reference Materials by Portable XRF Spectrometry: Implications for Uncertainty of Reference Values. Geo Stand. Geo Anal. Res. 41, 459–473. https://doi.org/10.1111/ggr.12162.

Rousaki, A., Coccato, A., Verhaeghe, C., Clist, B.O., Bostoen, K., Vandenabeele, P., Moens, L., 2016. Combined spectroscopic analysis of beads from the tombs of Kindoki, Lower Congo Province (Democratic Republic of the Congo). Appl. Spectrosc. 70, 76–93.

Sayre, E.V., Smith, R.W., 1967. Some materials of glass manufacturing in antiquity. In: Levey, M. (Ed.), Archaeological Chemistry: A Symposium, 3rd Symposium on Archaeological Chemistry. University of Pennsylvania Press, Philadelphia, pp. 279–312.

Schweizer, F., Rinuy, A., 1982. Manganese black as an Etruscan pigment. Stud. Conserv. 27, 118–123.

Simsek, G., Colomban, Ph., Wong, S., Zhao, B., Rougeulle, A., Liem, N.Q., 2015. Toward a fast non-destructive identification of pottery: the sourcing of 14th-16th century Vietnamese and Chinese ceramic shards. J. Cult. Heritage 16, 159–172.

Shortland, A., Schachner, L., Freestone, I., Tite, M., 2006. Natron as a Flux in the Early Vitreous Materials Industry: Sources, Beginnings and Reasons for Decline. J. Archaeol. Sci. 33, 521–530.

Smith, A.K., 1970. The struggle for the control of Southern Mozambique, Ph.D. Thesis, University of California.

Stern, W.B., Gerber, Y., 2004. Potassium-Calcium glass: new data and experiments. Archaeom. 46, 137–156.

Theal, G.M., 1902. The beginning of South African history. T. Fisher Unwin, London.

Tite, M.S., Shortland, A., Maniatis, Y., Kavoussanaki, D., Harris, S.A., 2006. The Composition of the soda-rich and mixed alkali plant ashes used in the production of glass. J. Archaeol. Sci. 33, 1284–1292.

Tournié, A., Prinsloo, L.C., Colomban, Ph., 2012. Raman classification of the glass beads excavated on Mapungubwe hill and K2, two archaeological sites in South Africa. J. Raman Spectrosc. 43, 532–542.

Ulitzka, S., 1994. Analysen von historischen Gläsern – Licht im Dunkel der Geschichte? In: Theuerkauff-Liederwald, A. (Ed.), Venezianisches Glas der Kunstsammlungen der Veste Coburg.

Die Sammlung Herzog Alfreds von Sachsen-Coburg und Gotha (1844-1900): Venedig, á la façon-de-Venise, Spanien, Mitteleuropa, Luca verlag, Lingen, pp. 40–53.

Van der Sleen, W.G.N., 1967. A Handbook on Beads. George Shumway, York, Pennsylvania.

Verità, M., 2013. Venetian soda glass. In: Janssens, K. (Ed.), Modern Methods for Analysing Archaeological and Historical Glass. Wiley, Chichester, pp. 515–536.

Verità, M., Zecchin, S., 2009. Thousand years of Venetian glass: the evolution of chemical composition from the origins to the 18th century. In: Janssens, K., Degryse, P., Cosyns, P., Caen, J., Van't dack L. (Eds.), Annales du 17e Congrès de l'Association Internationale pour l'Histoire du Verre (AIHV), Belgium, 4th to 8th September 2006. Aspeditions, Antwerp, pp. 602-613.

Wood, M., 2008. Post-European contact glass beads from the southern African interior: a tentative look at trade, consumption and identities. In: Swanepoel, N., Esterhuysen, A., Bonner, P. (Eds.), Five hundred years rediscovered. Witwatersrand University Press, Johannesburg, pp. 183–196.

Wood, M., 2011. A glass bead sequence for Southern Africa from the 8th to the 16th century AD. J. Afr. Archaeol. 9, 67–84.

Wood, M., Dussubieux, L., Robertshaw, P., 2012. Glass finds from Chibuene, a 6th to 17th century AD port in southern Mozambique. S. Afr. Archaeol. Bull. 67 (195), 59–74.

Zhao, H.X., Li, Q.H., 2017. Combined spectroscopic analysis of stratified glass eye beads from China dated to the Warring States Period. J. Raman spectrosc. 48, 1103–1110. https://doi.org/10.1002/jrs.5177.